Hippocampal CA1 spiking during encoding and retrieval: Relation to theta phase ☆

Joseph R. Manns, Eric A. Zilli, Kimberly C. Ong, Michael E. Hasselmo,
Howard Eichenbaum *

Center for Memory and Brain, Boston University, Boston, MA 02215, USA

Abstract

The hippocampal theta rhythm is a prominent oscillation in the field potential observed throughout the hippocampus as a rat investigates stimuli in the environment. A recent computational model [Hasselmo, M. E., Bodelon, C., & Wyble, B. P. (2002a). A proposed function for hippocampal theta rhythm: separate phases of encoding and retrieval enhance reversal of prior learning. *Neural Computation, 14*, 793–817. Neuromodulation, theta rhythm and rat spatial navigation. *Neural Networks, 15*, 689–707] suggested that the theta rhythm allows the hippocampal formation to alternate rapidly between conditions that promote memory encoding (strong synaptic input from entorhinal cortex to areas CA3 and CA1) and conditions that promote memory retrieval (strong synaptic input from CA3 to CA1). That model predicted that the preferred theta phase of CA1 spiking should differ for information being encoded versus information being retrieved. In the present study, the spiking activity of CA1 pyramidal cells was recorded while rats performed either an odor-cued delayed nonmatch-to-sample recognition memory test or an object recognition memory task based on the animal's spontaneous preference for novelty. In the test period of both tasks, the preferred theta phase exhibited by CA1 pyramidal cells differed between moments when the rat inspected repeated (match) and non-repeated (nonmatch) items. Also in the present study, additional modeling work extended the previous model to address the mean phase of CA1 spiking associated with stimuli inducing varying levels of retrieval relative to encoding, ranging from novel nonmatch stimuli with no retrieval to highly familiar repeated stimuli with extensive retrieval. The modeling results obtained here demonstrated that the experimentally observed phase differences are consistent with different levels of CA3 synaptic input to CA1 during recognition of repeated items.
© 2006 Elsevier Inc. All rights reserved.

Keywords: Hippocampus; Entorhinal; Theta; Model; Memory; Oscillation

The hippocampus (defined here as CA fields, dentate gyrus, and subiculum) supports the capacity for declarative memory in collaboration with the adjacent entorhinal, perirhinal, and postrhinal (parahippocampal in primates) cortices (Brown & Aggleton, 2001; Eichenbaum, 2000; Squire, Stark, & Clark, 2004). In humans, declarative memory is often expressed though the conscious recollection of facts and events (Gabrieli, 1998; Manns & Squire, 2002; Schacter, 1997). In other mammals, declarative memory is typically characterized as being spatial, temporal, associative, or rapidly acquired (Burgess, Becker, King, & O'Keefe, 2001; Eichenbaum & Cohen, 2001; Morris, 2001; O'Reilly & Rudy, 2001).

An important area of research has been the attempt to understand the computational principles of how the hippocampus interacts with adjacent cortical areas to support declarative memory (Hasselmo & McClelland, 1999; Lorincz & Buzsaki, 2000; McClelland, McNaughton, & O'Reilly, 1995; Nadel, Samsonovich, Ryan, & Moscovitch, 2000; O'Reilly & Rudy, 2001; Teyler & Discenna, 1986). One particularly compelling puzzle concerns how the

hippocampus attains a balance between encoding and retrieval processes. Presumably, the hippocampus participates in both encoding and retrieving memory, yet it is unclear how it does so in a way that optimally compares new and retrieved information without suffering from potentially incapacitating interference effects.

Some attempts to solve this puzzle have focused on the hippocampal theta rhythm (Hasselmo, 2005). The theta rhythm is a 4–12 Hz oscillation that is prominent in the local field potential recorded throughout the hippocampal region and is thought to play an important role in successful declarative memory (see Buzsaki, 2002 for a review). One possible role for the theta rhythm is that it appears to modulate the magnitude of synaptic currents at synapses in the hippocampus (Brankack, Stewart, & Fox, 1993; Orr, Rao, Houston, McNaughton, & Barnes, 2001; Wyble, Linster, & Hasselmo, 2000). This phase specificity of the theta rhythm differs across synapses of the hippocampus. In particular, the synaptic input from entorhinal cortex to CA1 is strongest at the troughs of the theta rhythm recorded at the hippocampal fissure and is weakest at the peaks of the fissure theta (Brankack et al., 1993). In contrast, the synaptic transmission from CA3 to CA1 is strongest at the peaks of the fissure theta and weakest at the troughs of the fissure theta (Brankack et al., 1993). In addition, different phases of theta rhythm are associated with differences in the induction of synaptic modification (Holscher, Anwyl, & Rowan, 1997; Hyman, Wyble, Goyal, Rossi, & Hasselmo, 2003; Pavlides, Greenstein, Grudman, & Winson, 1988). For example, in awake, behaving rats, stimulation in stratum radiatum of CA1 led to either long-term potentiation (LTP) or long-term depression (LTD), depending on whether the stimulation was applied at the peaks or troughs of the locally recorded theta rhythm (Hyman et al., 2003; also see McCartney, Johnson, Weil, & Givens, 2004 for a similar result).

Based on these physiological results, a computational model was recently proposed to describe how the theta rhythm might reflect the network dynamics that allow the hippocampus to oscillate rapidly between conditions promoting encoding and conditions promoting retrieval (Hasselmo, Bodelon, & Wyble, 2002a; Hasselmo, Hay, Ilyn, & Gorchetchnikov, 2002b). The model demonstrates that the best retrieval of memories occurs if, over the course of each theta cycle, the hippocampus transitions from strong input from entorhinal cortex to strong internal retrieval (see Fig. 1). In particular, the model specified that best performance occurs if input to CA1 would predominantly come from entorhinal cortex at the trough of fissure theta but would instead mainly come from CA3 at the peak of the fissure theta. The initial model focused on plasticity and synaptic transmission and did not derive results for spiking activity. However, a direct extension of the model predicts that the preferred theta phase of CA1 spiking should also differ between moments of strong encoding and strong retrieval. In the original version of the model (Hasselmo et al.,
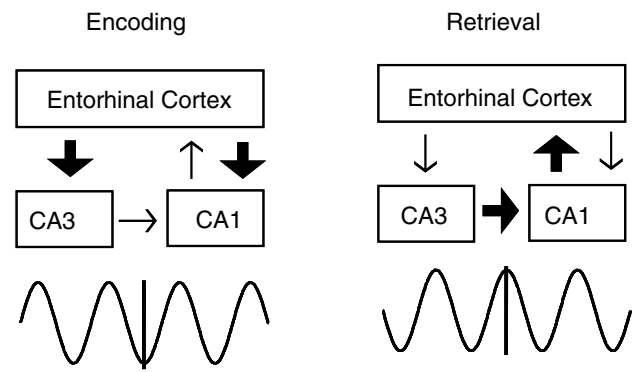

Fig. 1. Model of hippocampal network during encoding and retrieval (see text for details). During encoding, strong synaptic input from entorhinal cortex reaches CA1 and CA3 near the trough of the theta rhythm recorded at the hippocampal fissure. During retrieval, strong synaptic input from CA3 reaches CA1 near the peak of fissure theta.

2002a, 2002b), the maximum synaptic input to CA1 from entorhinal cortex was described as being 180 degrees out of phase from the maximum synaptic input from CA3. Yet whether or not the spiking activity of CA1 would also differ by 180 degrees between moments of strong encoding and strong retrieval was not specified.

The prediction that the preferred theta phase of CA1 spiking should differ between strong encoding and strong retrieval was tested in the current study using two recognition memory protocols. The activity of CA1 pyramidal cells was recorded while rats performed either a novel object exploration task (Experiment 1) or an odor-cued delayed nonmatch to sample (DNMS) task (Experiment 2). We reasoned that inspection of any item would likely elicit some degree of encoding and some degree of retrieval, regardless of whether the item was entirely novel or was very familiar. The objective of our analyses was therefore to compare the preferred theta phase of CA1 spiking between two conditions that differed only in the proportion of encoding and retrieval that would be expected to occur. Thus, the preferred phase of theta at which cells tended to spike was compared during the test period of each experiment between instances when the rat encountered a repeated odor (or object) and instances in which the rat encountered a non-repeated odor (or object). The idea was that inspection of a repeated item would bias activity in the hippocampus towards retrieval of the memory of that previously experienced item whereas inspection of a novel item would bias activity towards encoding the new information. Importantly, during the test period, the rat's overt behavior and expectations were constant as it began sampling of both the novel and familiar items. This consistency in behavior and expectancy would not be available in comparisons between items encountered during the sample period and test period. In both experiments, a difference in preferred theta phase between conditions was observed for CA1 spiking. However, the observed difference in phase for spiking activity was relatively small and was less than the theoretical maximum of 180 degrees. In the third section

of the present study, results for the preferred phase of CA1 spiking were derived from the computational model and were directly compared to the experimental results. The results of the model matched the experimental results and indicated that the theta phase offset of CA1 spiking activity between encoding and retrieval is much less than the phase offset of the incoming synaptic transmission from entorhinal cortex and CA3.

1. Experiment 1

1.1. Method

1.1.1. Procedure

Three male Long–Evans rats (>400 g) were familiarized with the testing chamber for at least 3 days prior to undergoing surgery to implant a recording headstage above the left dorsal hippocampus (3.6 mm posterior and 2.6 mm lateral to bregma). The recording headstage contained from 6 to 12 independently movable tetrodes aimed at CA1. Each tetrode was composed of four 12.5 μm nichrome wires whose tips were plated with gold to bring the impedance to 200 kΩ at 1 kHz. Animals were allowed to recover for 4–6 days, and the tetrodes were then moved down slowly, over the course of 1–2 weeks, until the tips reached the pyramidal cell layer of CA1. The tetrodes were screened each day for unit activity, and behavioral testing was administered on a day in which numerous CA1 pyramidal cells appeared across several tetrodes. The placement of the tetrode tips was verified by several CA1 pyramidal electrophysiological hallmarks (complex spikes, theta-modulated spiking, multi-unit bursts accompanied by 200 Hz "ripples" in the field potential) and by histology. One tetrode was lowered below the pyramidal layer to record theta near the hippocampal fissure. During testing, spike activity (10,000×, 600–6000 Hz) and local field potentials (1500×, 1–400 Hz) were amplified, filtered, and saved for offline analysis (DataWave Technologies).

Each trial of the novel object task consisted of a 5-min study period, a 5-min delay, and a 5-min test period. The rat remained in the recording chamber (0.76 m by 0.38 m wooden enclosure with 0.43 m high walls) throughout testing, including a 2-min inter-trial interval. The stimuli were a collection of plastic, wood, or metal junk objects or toys that were typically larger than $10 \times 10 \times 10$ cm but smaller than $17 \times 17 \times 17$ cm. Rats were not exposed to the objects prior to the testing session. At the beginning of the study period, two identical copies of an object were placed in opposite corners of the chamber. The start positions of the objects were counterbalanced such that half the time the objects were initially placed in the north and south corners and the other half the time the objects were placed in the east and west corners. After 1.25 min, and again at 2.5 and 3.75 min, both objects were moved in unison to the corner immediately clockwise to their previous position (e.g., objects in the north and south cor-

ners moved to the east and west corners, respectively). After the 5-min study period, the objects were removed from the enclosure, and a 5-min delay period followed. At the beginning of the test period, two objects were placed in opposite corners of the chamber. One object was a third copy of the object presented during the study period and the other object was a novel object. The initial positions of the objects were counterbalanced such that the repeated and novel objects were equally likely to appear in each of the four corners. The objects were moved to clockwise corners at each 1.25-min interval as in the study period. Rats were tested until they completed 10 trials or until they spent less than 10 s investigating objects during study period. Prior to the testing session, objects were paired on the basis of size and were randomly assigned to serve as either the repeated or novel object.

1.1.2. Data analysis

Behavioral performance was measured by frame-by-frame (30 frames/s) analysis of high-resolution digital video whose time stamps were synchronized with the acquisition of neural data. Time stamps were manually recorded when the rat initiated or terminated exploration of an object. A rat was considered to be exploring an object only if the animal was within 2 cm of the object and was showing evidence of active investigation (e.g., sniffing or directed attention).

Activity of individual units was obtained by separating the total activity from each tetrode by using software (Offline Sorter, Plexon Inc.) to define clusters of spikes determined by visually inspecting several waveform characteristics across the four wires (e.g., spike amplitude or waveform shape). A measure of the phase of hippocampal theta was obtained for every spike from the field potential of a tetrode that was placed near the hippocampal fissure. The theta phase was calculated by first finding the troughs of each cycle though an iterative search for local minima in the field potential filtered at 4–12 Hz. Differences between rats in the exact placement of the probe near the hippocampal fissure led to differences in the absolute phase of theta obtained for the overall mean phase of CA1 spiking, irrespective of differences between preferred phase for repeated and novel object. Although the questions of interest centered on the relative differences between mean theta phase of spiking for repeated versus novel items, an attempt was made to compare the results from animal to animal. In particular, an estimate of the depth of the tetrode near the fissure was determined by calculating the degree to which the theta from that tetrode was out of phase from the theta obtained from one of the tetrodes in the pyramidal layer. This depth estimate was used to adjust the theta phase measurements such that a phase value of 0 corresponded to the absolute peak of theta recorded at the fissure. This procedure involved a simple addition to the mean theta phase for both the novel and repeated objects, and differences in phase between conditions were unaffected by this procedure.

1.2. Results

During the test period, the three rats tended to spend more time inspecting the novel objects than inspecting the repeated objects, suggesting that they retained memory for the repeated objects (mean percent of time exploring novel objects ±95% confidence interval = 59.1 ± 8.4%). This proportion of time spent exploring the novel objects is similar to previous results (e.g., Ennaceur & Delacour, 1988; Clark, Zola, & Squire, 2000). Nevertheless, it is possible that an even greater proportion of time spent inspecting the novel object might have led to greater differences in terms of the preferred theta phase during inspection of repeated and novel objects. On the day of testing, a total of 34, 21, and 22 CA1 pyramidal cells were recorded for rats 1, 2, and 3, respectively.

The preferred phase of theta was analyzed for each unit and for population data (all pyramidal units combined) using standard circular statistics (Fisher, 1993). In particular, the mean phase of spikes recorded while the rat inspected repeated objects was compared to the mean phase of spikes recorded while the rat inspected novel objects using the Watson–Williams F test for circular means (Fisher, 1993). Only those units for which more than 10 spikes were recorded during inspection of both repeated and novel objects were included in the analyses of phase preference for individual units (15, 10, and 16 units for rats 1, 2, and 3, respectively). Of these 41 cells, 16 differed significantly ($p < .05$) in their preferred phase of theta between

instances of sniffing repeated and novel objects. Although the number of active cells and the number of statistically significant cells are relatively small, 39% (16/41) of the cells assessed show a significant phase difference between conditions biased towards encoding or retrieval, substantially more than the 5% that would be expected by chance at an alpha level of 0.05.

The prediction from the computational model that CA1 spiking activity should differ between moments of inspection of repeated and novel objects holds not only for individual neurons but also for the population activity of pyramidal cells. Accordingly, we next considered whether, for each rat, the combined activity of all pyramidal cells would show a difference in preferred theta phase between instances of inspecting repeated objects as compared to instances of inspecting novel objects. Fig. 2 shows three pairs (repeated vs. novel) of circular histograms, one pair for each of the three rats. For each of the three rats, the difference in preferred phase between conditions was greater than chance, although it was less than the maximal 180 degrees (difference = 40.2, 18.4, and 12.3 degrees for rats 1, 2, and 3, respectively; all $ps < .05$). In contrast, the average firing rate of the population activity and the average theta frequency and theta power were similar between conditions for each rat (see Fig. 2b–d). One possibility for why the observed difference for each rat was below the maximal 180 degrees was that using data from novel objects from the entire test period reduced the difference in memory strength between repeated
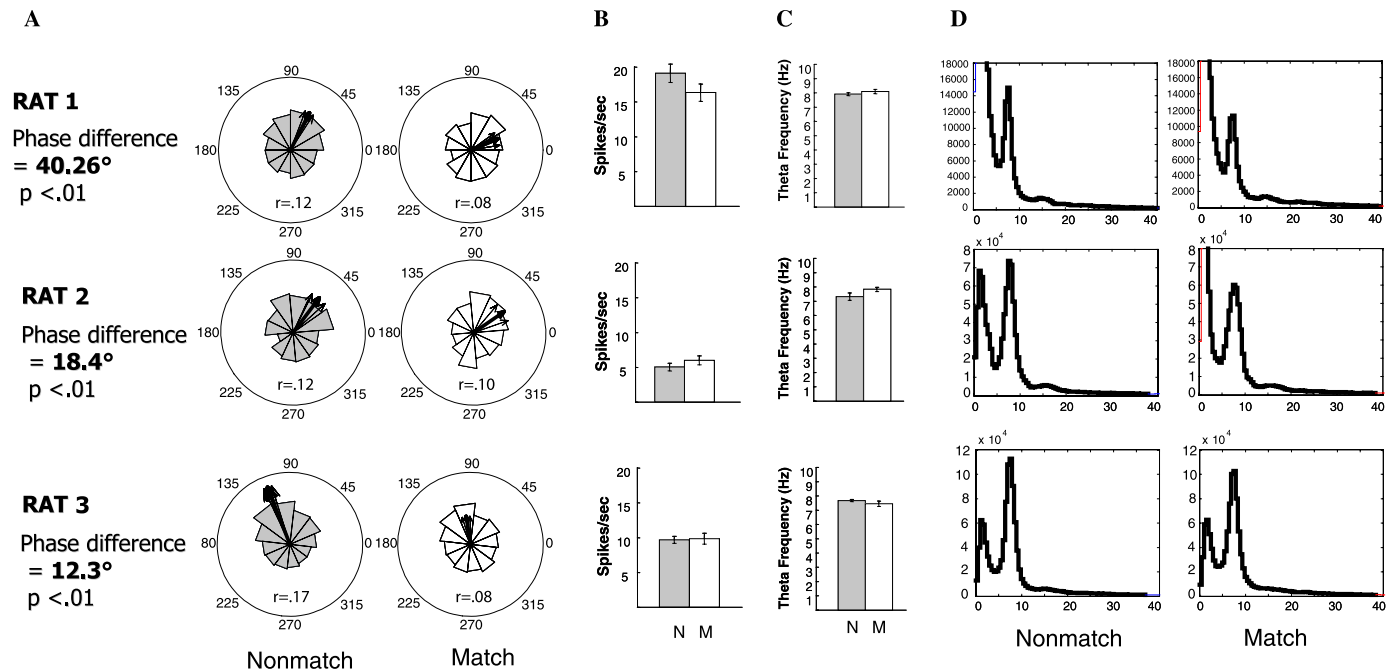

Fig. 2. (A) Preferred phase of CA1 spiking during inspection of novel (nonmatch) and repeated (match) objects by three rats during a novel object recognition memory task. The circular histograms show the distribution of phases. The length (r) of the mean resultant vector (thick arrow) is shown inside each circle. The radius of each circle corresponds to a length of 0.2. Thin arrows show the circular standard error of the mean direction. For all three rats, the mean phase of CA1 spiking differed between novel and repeated objects ($ps < .01$; Watson–Williams F-test). In contrast, the firing rate (B), theta frequency (C), and theta power (D) were similar for moments of inspecting novel and repeated objects. N = nonmatch; M = match.

and novel objects. That is, by the end of each test period, the novel object had been thoroughly inspected and was no longer novel. We therefore next considered the possibility that the phase preference of CA1 cells might change rather quickly in response to the initial inspection of a novel object. Fig. 3 shows data from the first 9 s of exploration of novel objects during the test period for each of the three rats. Data were analyzed from only those trials for which each rat spent at least 9 consecutive seconds inspecting the novel object upon first encountering it, and the population results are plotted in 3 s time bins. For each rat, the preferred theta phase shifted across the three time bins, suggesting that the phase at which CA cells were spiking corresponded to the amount of time the animal had spent investigating the novel object. For each rat, the difference in preferred phase was significantly different for the first 3 s of exploration as compared to seconds 6 to 9 (difference = 38.7, 165.7, and 58.4 degrees; $ps < .05$).

Although the analyses focused on the comparison between repeated and novel objects inspected during the test period, we also considered CA1 spiking activity during inspection of objects during the sample period. For all three rats, the preferred theta phase recorded during sampling of the novel objects in the sample period was similar to the preferred theta phase recorded during sampling of novel objects during the test period but differed significantly (all $ps < .05$) from the preferred theta phase recorded during sampling of repeated objects during the test period

(mean phase ± SEM for sample, novel, and repeated objects. Rat 1 sample = 51.98 ± 6.53, novel = 62.8 ± 6.3, and repeated = 22.6 ± 12.9; Rat 2 sample = 47.39 ± 6.12, novel = 52.9 ± 10.6, and repeated = 34.5 ± 14.9; Rat 3 sample = 108.48 ± 4.49, novel = 111.1 ± 3.9, and repeated = 98.8 ± 7.9). In addition, for the initial inspection of the novel objects during the sample period, the preferred theta phase differed significantly between the first 3 s of exploration as compared to seconds 6 to 9 for rat 1 ($p < .001$) and differed marginally for rat 3 ($p = .06$). However, this comparison was limited by the fact that rats usually did not spend at least nine consecutive seconds exploring a single sample object during their first exposure. Instead, rats usually divided their time between the two identical copies of the sample object during the sample period.

The results of Experiment 1 indicated that the preferred phase of CA1 spiking activity differed between occasions in which rats inspected novel and repeated objects, although the difference was much smaller than the maximum of 180 degrees. To explore this phase difference further, a separate group of rats were tested on another standard recognition memory test, the delayed nonmatch to sample test. The question of interest was whether the theta phase of CA1 spiking would differ between periods of inspection of repeated (match) and non-repeated (nonmatch) items, and whether the magnitude of this difference would be similar to the results obtained in Experiment 1.
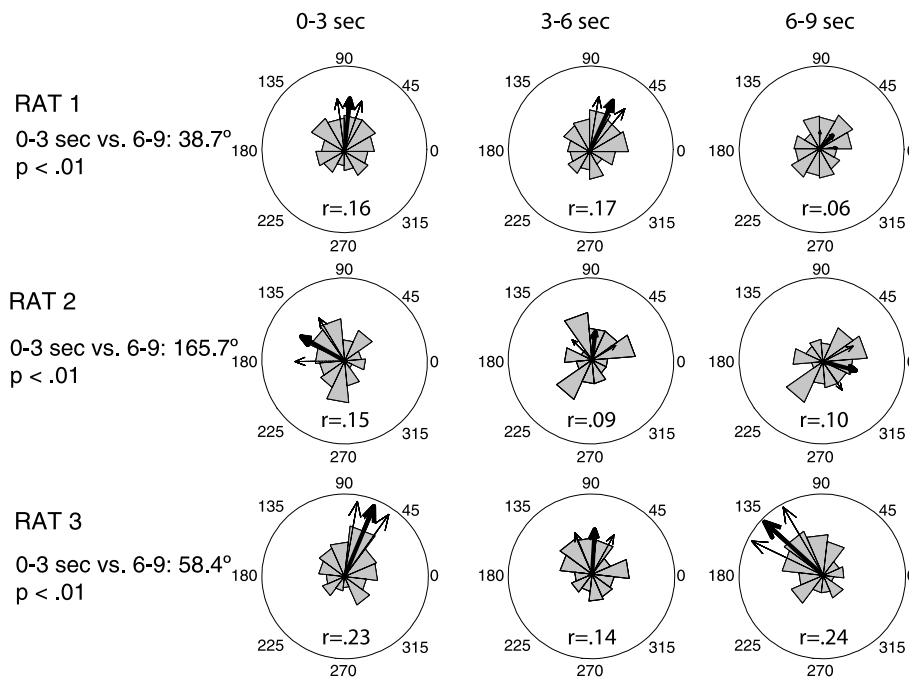

Fig. 3. Preferred phase of CA1 spiking during the initial 9 s of inspection of novel objects during the test period. The phase plots are shown separately in 3-s time intervals. The circular histograms show the distribution of phases. The length (*r*) of the mean resultant vector (thick arrow) is shown inside each circle. The radius of each circle corresponds to a length of 0.25. Thin arrows show the circular standard error of the mean direction. The difference in phase across the first 9 s of exploration (0–3 s vs. 6–9 s; all $ps < .01$) suggested that the preferred phase of theta quickly reflected familiarity with an object.

2. Experiment 2

2.1. Method

2.1.1. Procedure

Four male Long–Evans rats (>400 g) were trained on an odor-cued version of a delayed nonmatch to sample task. Rats completed all training and subsequent recording sessions in a rectangular wooden enclosure (0.76 m by 0.38 m with 0.43 m high walls). Each trial included a sample period, a brief (15 s) delay, and a test period. In the sample period, rats were presented with a ceramic pot (11 cm diameter, 10 cm high) that contained a small piece of sweetened cereal buried in sand that was scented with one of 10 possible household spices. After digging in the sand to retrieve the reward, the animal was held in one half of the enclosure by an inserted divider for the duration of the delay period. For the test period, two new pots containing scented sand were placed together on the opposite half of the enclosure in one of the two possible corners (corner position and left/right position were counterbalanced). One pot was scented with the same odor that was used in the sample period. The other pot was scented with one of the other nine odors not used in the sample period and contained a piece of sweetened cereal. At the end of the delay period, the divider was removed and the animal was allowed to dig in either pot. If the rat dug first in the non-matching (correct) odor, the pots were left in the enclosure until the rat retrieved the buried reward. If the rat dug first in the matching (incorrect) odor, the pots were immediately removed from the enclosure. A rat was considered to have made a digging choice when it made any contact with the sand with either its snout or paws. Trials were separated by a 30 s inter-trial interval. Testing continued until the rat completed 40 trials or until the rat refused to dig for rewards.

After rats achieved a criterion of three consecutive days of testing with better than 80% correct performance, rats were scheduled for surgery to implant a recording head-stage. The details of the surgery and post-surgery recording procedure were identical to those in Experiment 1.

2.1.2. Data analysis

Neural and behavioral data were recorded on days when activity from CA1 pyramidal cells was present on several tetrodes. In order to avoid repeated sampling of particular neurons, data were analyzed for each rat for the day on which the most pyramidal cells were recorded in a single testing session. Behavior was recorded with high-resolution digital video (30 frames per second) that was synchronized with the acquisition of neural data, and timestamps were obtained for match (during the test period, sniffing sand scented with an odor encountered in the previous sample period) and nonmatch (during the test period, sniffing sand scented with an odor not presented in the previous sample period) events. The beginning of each event was defined as the video frame on which the rat's nose was first within

1 cm of the pot. Rats typically spent less than 1 s (but more than .5 s) sniffing each pot, and therefore each event was considered to last .5 s. Individual spikes were assigned to different units and were assigned a theta phase (0–359 degrees) as in Experiment 1.

2.2. Results

Rats performed well during the recording sessions (mean percent correct ± SEM = 80.6 ± 6.6%). On the recording day, the activity from a total of 51 units was recorded (18, 6, 10, and 17 from rats 1, 2, 3, and 4, respectively). Due to the short (.5 s) time interval for the behavioral events and to the generally low firing rates of CA1 pyramidal cells, a number of the recorded cells emitted very few spikes during the events of interest. Thus, analysis of theta phase relationships could be analyzed for only the subset (14 of 51) of recorded cells that emitted more than 10 spikes during both the match and nonmatch events. Of these 14 cells, four differed significantly ($p < .05$) in their preferred phase of theta between instances of sniffing repeated and novel objects. The number of individual cells involved in this analysis is small, and further studies will be aimed at recording larger numbers of individual units. Nevertheless, the results of the single-unit analysis in this experiment were similar to those obtained in Experiment 1. That is, 4 of the 14 cells assessed (29%) showed a significant phase difference between conditions biased towards encoding or retrieval. In addition, the results of the single-unit analysis are consistent with the results of the population analysis, which are described next.

As in Experiment 1, we also considered for each rat whether the population spiking activity showed different preferred phases of theta for conditions biased towards retrieval (match) and encoding (nonmatch). Thus, the activity for all pyramidal cells was combined for each rat. Fig. 4 shows the population data for all four rats. For all four rats, the preferred phase of theta for spiking activity differed significantly ($p < .01$) between match and nonmatch events (Watson–Williams F test). Similar to the findings from Experiment 1, the magnitude of the difference was modest (difference = 34.2, 68.4, 35.5, and 91.7 degrees for rats 1, 2, 3, and 4, respectively). In addition, an unexpected result was that the direction of the difference (clockwise vs. counterclockwise) between match and nonmatch stimuli varied from rat to rat. Thus, the match–nonmatch difference was negative for rats 1 and 3 and positive for rats 2 and 4. A possible explanation for this finding is offered in the context of the results of modeling in Section 3.

3. Summary of experiments 1 and 2

The results of both Experiment 1 and Experiment 2 indicate that the preferred theta phase of CA1 spiking differs between conditions biased toward encoding and conditions biased towards retrieval. This result was observed for both
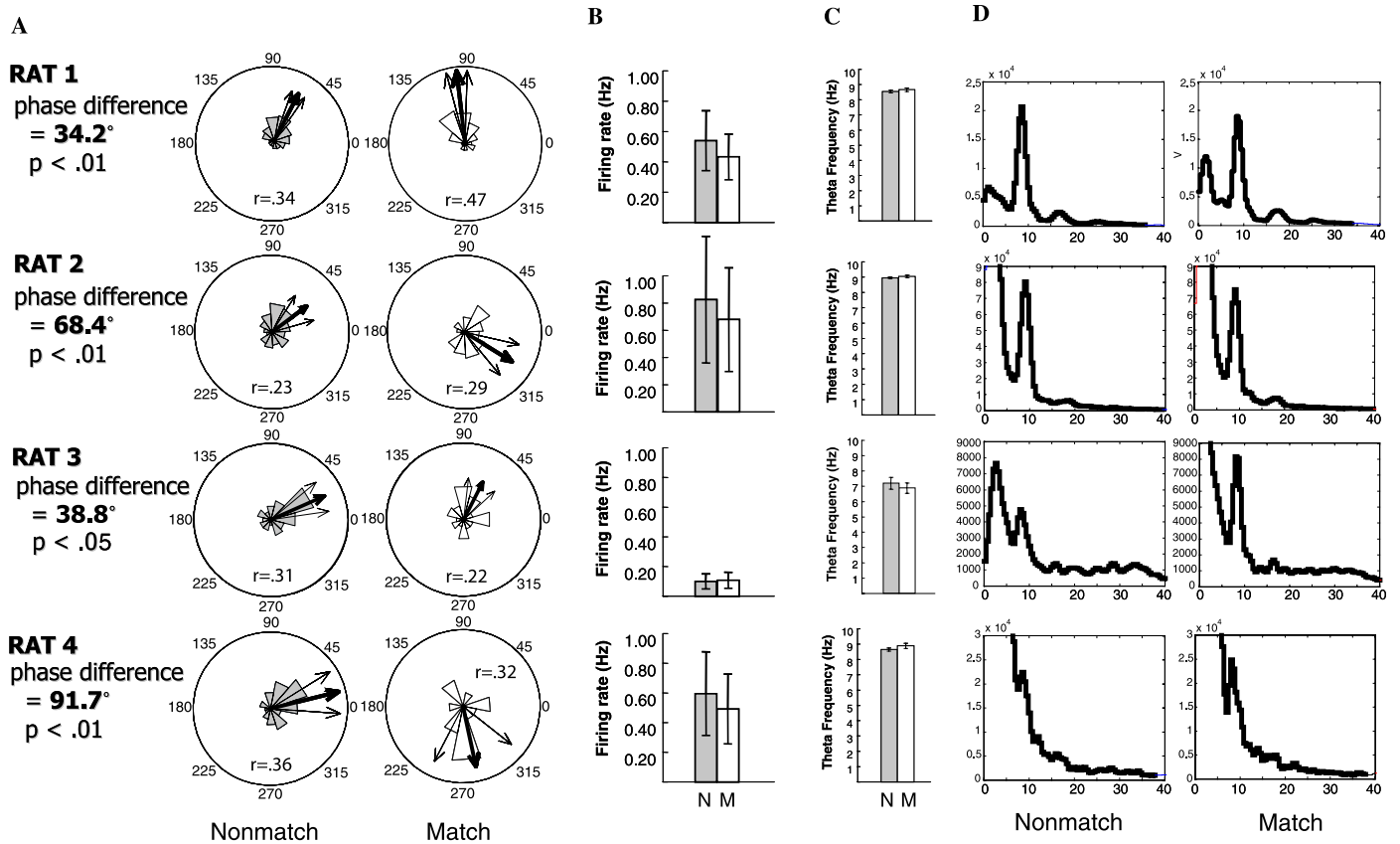
Fig. 4. (A) Preferred phase of CA1 spiking during inspection of non-repeated (nonmatch) and repeated (match) objects by four rats during a delayed nonmatch to sample recognition memory task. The circular histograms show the distribution of phases. The length (r) of the mean resultant vector (thick arrow) is shown inside each circle. The radius corresponds to a length of 0.5 for rat 1 and 0.4 for rats 2, 3, and 4. Thin arrows show the circular standard error of the mean direction. For all four rats, the mean phase of CA1 spiking differed between novel and repeated objects (ps < .05; Watson–Williams F-test). In contrast, the firing rate (B), theta frequency (C), and theta power (D) were similar for moments of inspecting non-repeated and repeated objects. N = nonmatch; M = match.

individual pyramidal cells and for the combined population activity of all pyramidal spiking. One notable feature of the results was that the magnitude of the difference in phase was much less than the maximal 180 degrees (range of differences from Experiments 1 and 2 = 12.3–91.7 degrees). The phase difference was also less than the 147 degrees that might have been expected on the basis of a previous current source density analysis that indicated a 147-degree difference between the phase of maximal entorhinal input to CA1 and the maximal CA3 input to CA1 (Brankack et al., 1993). A second notable feature of the results was that the direction (clockwise vs. counter-clockwise) of the theta phase difference was not always consistent from animal to animal. We therefore next compare the experimental results to new results obtained from the computational model. Previous reports of results from the model (Hasselmo et al., 2002a, 2002b; Hasselmo & Eichenbaum, 2005; Judge & Hasselmo, 2004) focused on either synaptic transmission or on LTP and LTD and did not obtain results for spiking activity. Here, we focus on new results of the model directly relevant to the experimental results, the preferred theta phase of CA1 spiking activity during encoding and retrieval.

4. Model

4.1. Method

The computational model used here to obtain results for CA1 spiking activity is identical to the original, fully detailed model (Hasselmo et al., 2002a, 2002b), with one exception. The original model suggested that the maximal synaptic input from region CA3 to CA1 should be 180 degrees out of phase with synaptic input from entorhinal cortex to CA1. A subsequent revision of the model (Judge & Hasselmo, 2004) suggested that if the amount of long-term potentiation heavily outweighed the amount of long-term depression, the expected theta phase offset of synaptic input would be smaller. Analysis of optimal performance with only long-term potentiation suggests a phase difference of about 124 degrees. This smaller phase difference is consistent with an empirical current source density analysis of rhythmic changes in membrane currents in region CA1 of the hippocampus (Brankack et al., 1993), which showed that the maximal current from CA3 to CA1 differed from the maximal current from entorhinal cortex to CA1 by about 147 degrees. For the analysis presented

here, we have inserted into the original model the maximal phases of membrane currents estimated from the current source density data (Brankack et al., 1993). The full details of the model were published previously (Hasselmo et al., 2002a), and the most relevant aspects are summarized below.

The network was used to generate predictions about the relative phases of maximal spiking activity in region CA1 for match versus nonmatch odors in the delayed nonmatch to sample task. The physiological variables known to change over the course of a theta cycle were modeled as sinusoids with individual phase offsets which match the current source density data. Specifically, synaptic plasticity is represented as a sinusoid varying between −1 (LTD) and +1 (LTP):

$$\Theta_{\text{LTP}}(t) = \sin(t + \Phi_{\text{LTP}})$$

Strengths of afferent synaptic input to CA1 from ECIII and CA3 are modeled as positive shifted sinusoids that vary from 0 to 1:

$$\Theta_{\text{ECIII}} = \tfrac{1}{2} + \tfrac{1}{2}\sin(t + \Phi_{\text{ECIII}})$$

$$\Theta_{\text{CA3}} = \tfrac{1}{2} + \tfrac{1}{2}\sin(t + \Phi_{\text{CA3}})$$

Rhythmic changes in synaptic inhibition at the soma are modeled with a similar equation:

$$\Theta_{\text{Soma}} = \tfrac{1}{2} + \tfrac{1}{2}\sin(t + \Phi_{\text{Soma}})$$

The phases of these excitatory and inhibitory synaptic input functions were based on estimated phases from the current source density data (Table 1 column AC in Brankack et al., 1993) of 129 degrees for CA1 lacunosum-moleculare (EC excitatory currents), 276 degrees for CA1 radiatum (CA3 input), and 145 degrees for CA1 pyramidale (inhibitory currents). Note that the current source density estimates were based on the peak of the oscillation, whereas sine waves have peaks at 90 degrees. Therefore, 90 degrees were subtracted from the current source density such that the resulting phase offsets were as follows: $\Phi_{\text{LTP}} = 0, \Phi_{\text{ECIII}} = 39$ and $\Phi_{\text{CA3}} = 186$. Since the phase for CA1 pyramidale reported in Brankack et al. (1993) was for a current source, we add 180 degrees to find the phase of the corresponding sink: $\Theta_{\text{Soma}} = 325$. Fig. 5 shows how these physiological variables (shown in Fig. 5B) match the current source density data from Brankack et al. (1993) illustrated schematically (in Fig. 5C). In the model, the strength of Schaffer collateral synaptic input from region CA3 to region CA1 is represented by the matrix W. Input patterns consisted of binary vectors representing both unique (unshared) odor input and overlapping (shared) features of the context. Input patterns were given to both region CA3 (a_{CA3}) and region ECIII (a_{ECIII}). CA1 activity is then the sum of the inputs from CA3 and ECIII minus the inhibitory effect on the soma of pyramidale interneurons:

$$a_{\text{CA1}} = \Theta_{\text{CA3}}Wa_{\text{CA3}} + \Theta_{\text{ECIII}}a_{\text{ECIII}} - \Theta_{\text{Soma}}$$

To explore properties of the network for different sequences of input patterns, the network was trained on a number
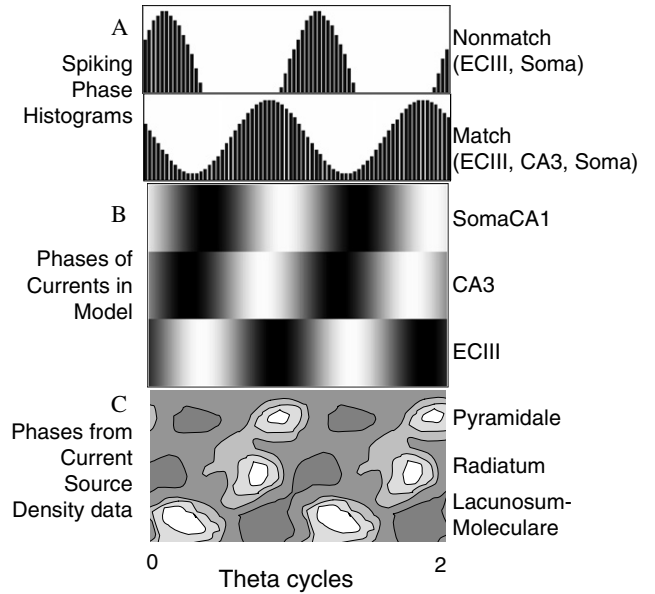

Fig. 5. (A) Spiking phase histograms from numerical simulations. In the nonmatch condition, no associations have been made over the Schaffer collaterals from CA3 to CA1, so only ECIII activity reflecting sensory input and rhythmic inhibition from local interneurons cause CA1 activity, resulting in a mean phase of 48°. In the match condition, the Schaffer collaterals have learned an association, so CA1 activity reflects both ECIII sensory input and CA3 learned association input, as well as inhibition, giving a mean phase of 291° and a phase difference between the conditions of 117°. (B) Data from the numerical simulations showing phases of maximal CA3 and ECIII input as well as peak depolarization of CA1 pyramidal somas. Phases of maximal CA3 and ECIII input were set to match the peaks of current sinks (white) found in current source density data from Brankack et al. (1993), (C).

of different input patterns with different amounts of overlap and different numbers of presentations. These explorations of responses to sequences of input patterns used synaptic modification of the Schaffer collaterals, with the following Hebbian learning rule:

$$\frac{\text{d}W}{\text{d}t} = \int \Theta_{\text{LTP}}a_{\text{CA1}}a_{\text{CA3}}^{T}\text{d}t$$

in which the LTP sinusoid causes the weight changes to vary from positive to negative. At the start of simulations, the matrix W had all zero elements. The sample period was simulated with a period of one or two cycles of rhythmic network activity, during which the sample stimulus was presented to both region CA3 and EC layer III. Synaptic modification was implemented at the end of the sample period on the basis of the activity during the sample period. The phase of spiking activity was then evaluated during separate test periods with input of the same vector used during the sample period (match) or with input of a different input vector (nonmatch). The examples shown in the figures presented here use synaptic weights with specific values described in the results section. A more detailed mathematical and computational analysis of spiking phases in the model will be published separately (Zilli and Hasselmo, in preparation).

4.2. Results

The results from the model resemble the experimental results in three important ways: (1) the phase of firing during match and nonmatch conditions differed, (2) the magnitude of phase difference in spiking was smaller than the phase difference in synaptic currents, and (3) the directionality of phase difference could vary depending on the number of previous presentations of odors. As shown in Figs. 5 and 6, similar to the experimental data, the model resulted in CA1 spiking that showed different mean phases of firing relative to theta for the match and nonmatch conditions. Fig. 5A shows the simplest example of this phase difference. The nonmatch odor shown on top only activates ECIII input, and has no overlap with previously modified weights W, therefore causing no CA3 input. This results in the mean phase of spiking in CA1 closely matching the peak phase of synaptic input from ECIII. In contrast, the match odor shown in the next row activates both ECIII input and synaptic input from CA3 (with strength W of 1.0). This results in spiking which combines the phases of ECIII and CA3 input, giving a mean phase of spiking for the match odor which differs from the mean phase of spiking induced by the nonmatch odor.

Like the experimental data, the difference in preferred phase of spiking between match and nonmatch conditions resulting from the model was smaller than the difference in phase of synaptic currents. In Fig. 5, the mean phase for the match odor differed from the mean phase of the nonmatch odor by 117 degrees, which is smaller than the difference of 147 degrees between the phase of maximal synaptic input to CA1 from entorhinal cortex versus CA3. The magnitude of spiking phase differences in the experimental data from Experiment 1 and Experiment 2 ranged from 12.1 to 91.7 degrees. If we assume ECIII input has constant strength 1.0 and the nonmatch stimulus does not activate CA3 input at all, then this range of phase differences corresponds to differences in relative strength of synaptic input associated with the match stimulus varying from about $W = 0.07$ to $W = 0.45$. More complex effects could be obtained with different amounts of previous learning of the match and nonmatch odors, which differ from the previous example by causing different amounts of overlap of nonmatch input with the previously modified synapses. In particular, the model provides a functional explanation for the different direction of phase differences observed in the experimental data. Fig. 6 shows results from two instances of the model, and the results from two rats (rats 1 and 2, Experiment 2) are presented in addition for comparison. As shown in the Fig. 6, with different relative amounts of learning of different odors, the model produced theta phase differences corresponding to either clockwise phase differences (e.g., Fig. 6, left) or counterclockwise phase differences (e.g., Fig. 6, right) in preferred theta phase between match and nonmatch conditions, similar to the experimental data. In that figure, W was set to different values to represent different amounts of previous learning of the match and nonmatch odors. For the clockwise shift case, the strength of ECIII input was set to 1 and the strength of W was set to 0.03 for nonmatch and 0.4
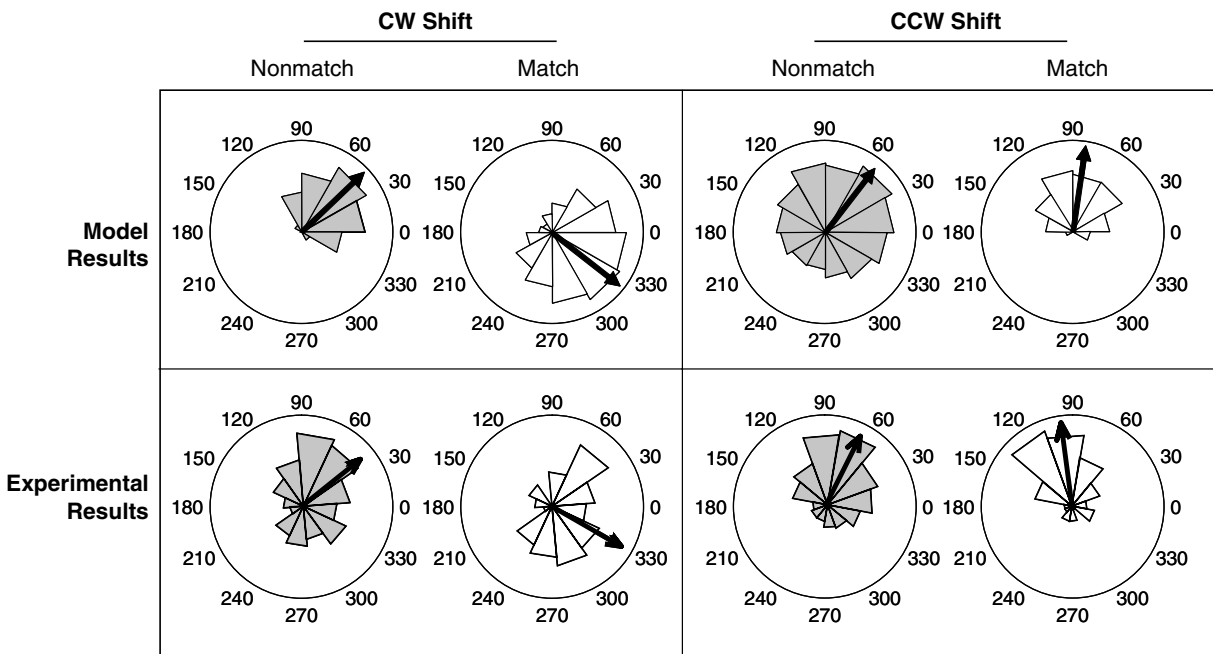

Fig. 6. Comparison of simulation output to experimental data for both shift directions under match and nonmatch conditions. Left. The simulation produces a clockwise phase difference of 82° between nonmatch (mean phase 44°) and match (mean phase 322°) conditions. The experimental data shows a clockwise phase difference of 69° between nonmatch (mean phase 37°) and match (mean phase 328°) conditions. Right. The simulation produces a counterclockwise phase difference of 29° between nonmatch (mean phase 53°) and match (mean phase 82°) conditions. The experimental data shows a counterclockwise phase difference of 34° between nonmatch (mean phase 62°) and match (mean phase 96°) conditions.

for match. The same change in W from 0.03 to 0.4 used in the clockwise case can cause a counterclockwise shift if the rat is assumed to have a different value of Φ_{CA3} which is less than about 130°. Alternately, the counterclockwise shift can be modeled with the strength of ECIII input set to 1.2 and the strength of W at 0.25 for nonmatch and 0.01 for match. These are just specific examples of possible relative amounts of prior exposure, but they demonstrate how different amounts of prior learning of the match and nonmatch odors can influence the relative phase difference between these cases.

5. Summary of model performance

The model produced results that were consistent with the experimental data in that in both cases the phase offset between encoding and retrieval conditions was relatively small and that in both cases clockwise and counterclockwise shifts were observed. The resulting small phase offsets from the model are understood by considering that most stimuli will typically elicit some amount of retrieval and some amount of encoding. Thus, CA1 spiking activity for any given stimulus would reflect synaptic input from both CA3 and entorhinal cortex, and the preferred theta phase of the CA1 spiking would fall somewhere in between the preferred theta phase of CA3–CA1 synaptic transmission and the preferred theta phase of entorhinal cortex-CA1 synaptic transmission. The preferred theta phase of CA1 spiking for a stimulus would therefore be closer to the preferred phase of entorhinal cortex synaptic transmission if the stimulus elicited less retrieval activity and would be closer to the preferred phase of CA3 synaptic transmission if the stimulus elicited proportionally more retrieval activity (more overlap with previous representations encoded with synaptic modification). Even in instances in which an entirely novel stimulus was compared to a repeated stimulus, a difference in preferred CA1 spiking occurred due to the fact that CA1 activity for the novel stimulus would reflect synaptic input from only entorhinal cortex whereas CA1 activity for the repeated stimulus would reflect synaptic input from both entorhinal cortex and CA3. Indeed, this instance of an entirely novel stimulus compared to a repeated stimulus is depicted in Fig. 5A.

The observation that the model, like the results from Experiment 2, showed both clockwise and counterclockwise theta phase offsets between encoding and retrieval conditions can be understood by considering that the preferred theta phase of CA1 spiking for a repeated stimulus reflects retrieval of not only the most recent encounter with the stimulus but also reflects some amount of retrieval for any other prior encounters. The schematic in Fig. 5A shows the simplest case of a match stimulus that had been encountered previously only once and a nonmatch stimulus that had never been encountered before. However, in Experiment 2 the match and nonmatch stimuli on each trial were odors drawn from a pool of only 10 odors. Thus, even within one day of testing, each stimulus was encountered

numerous times. In the model, when the amount of learning during a single presentation of a stimulus was small, the synaptic strengths grew slowly toward their maximum value and their strength reflected the total number of times an odor had been presented. For example, when the match and nonmatch odors had been encountered the same number of times on previous trials, then the preferred phase of CA1 spiking for the match odor was closer than that for the nonmatch odor to the phase of CA3 input because the activity for the match odor reflected retrieval of memory for the current trial in addition to memory from previous trials. In this instance, the CA1 activity for the nonmatch odor reflected memory only from previous trials. In contrast, when the nonmatch odor had been encountered more frequently than the match odor on previous trials, the amount of retrieval from previous trials sometimes outweighed the amount of retrieval from the current trial. In these instances, the preferred phase of CA1 spiking for the nonmatch odor was closer than that for the match odor to the phase of CA3 input because these instances reflected greater overall (current trial plus previous trials) memory retrieval for the nonmatch odor as compared to the match odor.

6. Discussion

Recent computational models of the hippocampus demonstrate that aspects of memory function are enhanced if synaptic input to CA1 alternates at the theta frequency between strong input from entorhinal cortex and strong input from CA3, allowing a rapid oscillation between processes of encoding and retrieval (Hasselmo et al., 2002a, 2002b; Hasselmo, 2005). The present study tested an extension of the model noting that CA1 spikes emitted during encoding conditions should occur at different phases than CA1 spikes emitted during retrieval conditions. The results from two recognition memory protocols were consistent with this prediction and indicated that the preferred theta phase of CA1 spiking differed between conditions biased towards encoding (inspecting a new nonmatching item) and conditions biased towards retrieval (inspecting a repeated match item). Results of CA1 spiking newly obtained from the model closely matched the experimental results.

The experimental data and the results from the model both indicated that the difference in preferred theta phase for repeated and non-repeated items was relatively small and was less than either the maximal 180 degrees or the 147 degrees suggested by the offset of synaptic input currents to CA1 from CA3 and entorhinal cortex (Brankack et al., 1993). The results from the model suggested that the small difference in mean phase for CA1 spikes occurred because most stimuli elicit some degree of both encoding and retrieval. For most stimuli considered in the model, the preferred theta phase of CA1 spiking fell somewhere between the phase of theta at which entorhinal synaptic input was strongest (reflecting encoding processes) and

the phase of theta at which CA3 synaptic input was strongest (reflecting retrieval processes). In the results of the model, repetition of an item within a trial shifted the mean phase of CA1 spiking toward the phase of CA3 input, reflecting an increased contribution of retrieval processes. However, the increased synaptic input from CA3 did not necessarily reduce the synaptic input from entorhinal cortex or reduce encoding of the repeated item. Thus, the results of the model suggested that repetition did not cause the preferred phase of CA1 spiking to align with the phase of maximal CA3 input but instead only shifted the mean phase of CA1 spiking towards the phase of CA3 input by an amount that was proportional to the strength of retrieval elicited by the repeated (match) item.

In the computational model, items that elicited no retrieval, such as entirely novel items, resulted in CA1 spiking whose phase was primarily influenced by the phase of maximal entorhinal cortex input. That is, although the model never resulted in CA1 spiking that reflected only retrieval, it was possible for the model to result in CA1 spiking that reflected only encoding. However, the example of an entirely novel stimulus eliciting no retrieval is most likely atypical. Indeed, even entirely novel stimuli are in principle capable of cueing other, related memories. Moreover, in Experiment 1 the theta phase of CA1 spiking that occurred during inspection of a novel stimulus changed over the first nine seconds of exploration (see Fig. 3). One possible interpretation of this result is that CA1 spiking quickly begins to reflect retrieval processes, even within the first few seconds of inspection. With these ideas in mind, it is possible that most encounters with stimuli, except for perhaps the first few seconds of inspecting a novel item that triggers no retrieved associations, will result in both encoding and retrieval processes. By this view, the mean phase of CA1 spiking will reflect the balance of encoding and retrieval and will typically fall between the two possible extremes.

The experimental data presented here are consistent with previous studies of the timing of spiking activity relative to theta rhythm oscillations in the hippocampal formation. In particular, the experiments had mean phases of firing relatively close to the peak of theta rhythm recorded at the fissure (reference phase zero). This is consistent with previous studies of spike firing relative to fissure theta (Fox, Wolfson, & Ranck, 1986; Skaggs, McNaughton, Wilson, & Barnes, 1996; Csicsvari, Hirase, Czurko, Mamiya, & Buzsaki, 1999) which finds strong phase selectivity of firing, with peak firing near the peak of fissure theta. However, previous studies did not compare phase of firing in different behavioral conditions such as match and nonmatch.

The experimental data presented here are also consistent with previous studies showing phase locking of hippocampal field activity during different behavioral states. If dynamics are appropriate for encoding or retrieval at different phases of theta, then network function could be enhanced by shifting theta phase to the encoding phase at the onset of a new stimulus being encoded, or by shifting the theta phase to the retrieval phase at the onset of a stimulus being retrieved. This is consistent with data showing phase locking of hippocampal theta rhythm to the encoding of new stimuli in a working memory task (Givens, 1996), as well as to whisker movements (Semba & Komisaruk, 1984) and sniffing (Macrides, Eichenbaum, & Forbes, 1982). The separation of encoding and retrieval phases is consistent with evidence that the induction of long-term potentiation shifts with stimulation relative to behaviorally induced phase locking (McCartney et al., 2004). In human subjects (Rizzuto, Madsen, Bromfield, Schulze-Bonhage, & Kahana, 2006), phase locking has been shown to differ between encoding of new sample stimuli and recognition of a test stimulus by magnitudes similar to the differences in phase of synaptic current used in the computational models (Judge & Hasselmo, 2004).

The computational modeling results presented here extend previous results focused on the phase of synaptic input during encoding and retrieval. The initial model showed that performance in a reversal task is optimal when the magnitude of afferent synaptic input from entorhinal cortex to CA1 and the induction of long-term potentiation is 180 degrees out of phase with the magnitude of transmission at associative synapses from CA3 to CA1 (Hasselmo et al., 2002a), and the magnitude of somatic depolarization (Hasselmo et al., 2002b). A later model constrained the synaptic modification to be all positive, and showed optimal function with smaller phase differences between EC and CA3 input, and with a phase offset between EC input and the induction of long-term potentiation consistent with experimental data on the induction of LTP relative to stimulation of stratum lacunosum-moleculare (Judge & Hasselmo, 2004). These previous models did not explicitly address the timing of spikes induced by synaptic currents, but the simulations presented here and further mathematical analysis (Zilli and Hasselmo, in preparation) show that CA1 spiking phase differences are smaller than synaptic phase differences and depend on relative amounts of previous encoding. The modeling results presented here suggest that CA1 spiking phase differences were smaller than synaptic phase differences because CA1 spikes were influenced by synaptic input from both CA3 and entorhinal cortex. In the model, items typically elicited both encoding and retrieval, and thus the spiking in CA1 was influenced by both CA3 input and entorhinal input. Accordingly, the mean theta phase for most items occurred somewhere between the phase of entorhinal input and the phase of CA3 input.

The experimental results presented here support the computational model and strengthen its tenability as a possible account of the network dynamics of encoding and retrieval in the hippocampus and entorhinal cortex. An important implication of the results and of the model is that the processes of encoding and retrieval are not accurately represented as discrete stages of memory. Instead, the results suggest that both processes may operate concurrently. By this view, the terms are perhaps best thought of

as labels for the extreme ends of a network fluctuation that occurs at theta frequency (from 4 to 10 times a second). The frequent perturbations of the network state towards one of the poles of encoding and retrieval might allow the hippocampus and entorhinal cortex to achieve a balance between binding associations and distinguishing different experiences. That is, the model describes a means for encouraging or discouraging spike-timing dependent plasticity in CA1 insofar as spikes representing incoming information and spikes representing retrieved memory are either brought closer together or pulled farther apart in time.

References

Brankack, J., Stewart, M., & Fox, S. E. (1993). Current source density analysis of the hippocampal theta rhythm: associated sustained potentials and candidate synaptic generators. *Brain Research, 615*, 310–327.

Brown, M. W., & Aggleton, J. P. (2001). Recognition memory: what are the roles of perirhinal cortex and hippocampus? *Nature Reviews Neuroscience, 2*, 51–61.

Burgess, N., Becker, S., King, J. A., & O'Keefe, J. (2001). Memory for events and their spatial context: models and experiments. *Philosophical Transactions of the Royal Society of London: Biological Sciences, 356*, 1493–1503.

Buzsaki, G. (2002). Theta oscillations in the hippocampus. *Neuron, 33*, 325–340.

Clark, R. E., Zola, S. M., & Squire, L. R. (2000). Impaired recognition memory in rats after damage to the hippocampus. *Journal of Neuroscience, 20*, 8853–8860.

Csicsvari, J., Hirase, H., Czurko, A., Mamiya, A., & Buzsaki, G. (1999). Oscillatory coupling of hippocampal pyramidal cells and interneurons in the behaving rat. *Journal of Neuroscience, 19*, 274–287.

Eichenbaum, H. (2000). A cortical-hippocampal system for declarative memory. *Nature Reviews Neuroscience, 1*, 41–50.

Eichenbaum, H., & Cohen, N. J. (2001). *From conditioning to conscious recollection: Memory systems of the brain*. New York: Oxford University Press.

Ennaceur, A., & Delacour, J. (1988). A new one-trial test for neurobiological studies of memory in rats. 1: Behavioral data. *Behavioral Brain Research, 31*, 47–59.

Fisher, N. I. (1993). *Statistical analysis of circular data*. Cambridge: Cambridge University Press.

Fox, S. E., Wolfson, S., & Ranck, JB. Jr., (1986). Hippocampal theta rhythm and the firing of neurons in walking and urethane anesthetized rats. *Brain Research, 62*, 495–508.

Gabrieli, J. D. (1998). Cognitive neuroscience of human memory. *Annual Review of Psychology, 49*, 87–115.

Givens, B. (1996). Stimulus-evoked resetting of the dentate theta rhythm: relation to working memory. *Neuroreport, 8*, 159–163.

Hasselmo, M. E. (2005). What is the function of hippocampal theta rhythm?—Linking behavioral data to phasic properties of field potential and unit recording data. *Hippocampus, 15*, 936–949.

Hasselmo, M. E., Bodelon, C., & Wyble, B. P. (2002a). A proposed function for hippocampal theta rhythm: separate phases of encoding and retrieval enhance reversal of prior learning. *Neural Computation, 14*, 793–817.

Hasselmo, M. E., & Eichenbaum, H. (2005). Hippocampal mechanisms for the context-dependent retrieval of episodes. *Neural Networks, 18*, 1172–1190.

Hasselmo, M. E., Hay, J., Ilyn, M., & Gorchetchnikov, A. (2002b). Neuromodulation, theta rhythm and rat spatial navigation. *Neural Networks, 15*, 689–707.

Hasselmo, M. E., & McClelland, J. L. (1999). Neural models of memory. *Current Opinion in Neurobiology, 9*, 184–188.

Holscher, C., Anwyl, R., & Rowan, M. J. (1997). Stimulation on the positive phase of hippocampal theta rhythm induces long-term potentiation that can be depotentiated by stimulation on the negative phase in area CA1 in vivo. *Journal of Neuroscience, 17*, 6470–6477.

Hyman, J. M., Wyble, B. P., Goyal, V., Rossi, C. A., & Hasselmo, M. E. (2003). Stimulation in hippocampal region CA1 in behaving rats yields long-term potentiation when delivered to the peak of theta and long-term depression when delivered to the trough. *Journal of Neuroscience, 23*, 11725–11731.

Judge, S. J., & Hasselmo, M. E. (2004). Theta rhythmic stimulation of stratum lacunosum-moleculare in rat hippocampus contributes to associative LTP at a phase offset in stratum radiatum. *Journal of Neurophysiology, 92*, 1615–1624.

Lorincz, A., & Buzsaki, G. (2000). Two-phase computational model training long-term memories in the entorhinal-hippocampal region. *Annals of the New York Academy of Sciences, 911*, 83–111.

Macrides, F. H., Eichenbaum, H., & Forbes, W. B. (1982). Temporal relationship between sniffing and limbic theta rhythm during odor discrimination reversal learning. *Journal of Neuroscience, 2*, 1705.

Manns, J. R., & Squire, L. R. (2002). The medial temporal lobe and memory for facts and events. In A. Baddeley, M. Kopelman, & B. Wilson (Eds.), *Handbook of memory disorders* (2nd Ed., pp. 81–99). West Sussex, England: John Wiley & Sons.

McCartney, H., Johnson, A. D., Weil, Z. M., & Givens, B. (2004). Theta reset produces optimal conditions for long-term potentiation. *Hippocampus, 14*, 684–687.

McClelland, J. L., McNaughton, B. L., & O'Reilly, R. C. (1995). Why there are complementary learning systems in the hippocampus and neocortex: insights from the successes and failures of connectionist models of learning and memory. *Psychological Review, 102*, 419–457.

Morris, R. G. (2001). Episodic-like memory in animals: psychological criteria, neural mechanisms and the value of episodic-like tasks to investigate animal models of neurodegenerative disease. *Philosophical Transactions of the Royal Society of London: Biological Sciences, 356*, 1453–1465.

Nadel, L., Samsonovich, A., Ryan, L., & Moscovitch, M. (2000). Multiple trace theory of human memory: computational, neuroimaging, and neuropsychological results. *Hippocampus, 10*, 352–368.

O'Reilly, R. C., & Rudy, J. W. (2001). Conjunctive representations in learning and memory: principles of cortical and hippocampal function. *Psychological Review, 108*, 311–345.

Orr, G., Rao, G., Houston, F. P., McNaughton, B. L., & Barnes, C. A. (2001). Hippocampal synaptic plasticity is modulated by theta rhythm in the fascia dentata of adult and aged freely behaving rats. *Hippocampus, 11*, 647–654.

Pavlides, C., Greenstein, Y. J., Grudman, M., & Winson, J. (1988). Long-term potentiation in the dentate gyrus is induced preferentially on the positive phase of theta-rhythm. *Brain Research, 439*, 383–387.

Rizzuto, D. S., Madsen, J. R., Bromfield, E. B., Schulze-Bonhage, A., & Kahana, M. J. (2006). Human neocortical oscillations exhibit theta phase differences between encoding and retrieval. *Neuroimage, 31*, 1352–1358.

Schacter, D. L. (1997). The cognitive neuroscience of memory: perspectives from neuroimaging research. *Philosophical Transactions of the Royal Society of London: Biological Sciences, 352*, 1689–1695.

Semba, K., & Komisaruk, B. R. (1984). Neural substrates of two different rhythmical vibrissal movements in the rat. *Neuroscience, 12*, 761–774.

Skaggs, W. E., McNaughton, B. L., Wilson, M. A., & Barnes, C. A. (1996). Theta phase precession in hippocampal neuronal populations and the compression of temporal sequences. *Hippocampus, 6*, 149–172.

Squire, L. R., Stark, C. E., & Clark, R. E. (2004). The medial temporal lobe. *Annual Review of Neuroscience, 27*, 279–306.

Teyler, T. J., & Discenna, P. (1986). The hippocampal memory indexing theory. *Behavioral Neuroscience, 100*, 147–154.

Wyble, B. P., Linster, C., & Hasselmo, M. E. (2000). Size of CA1-evoked synaptic potentials is related to theta rhythm phase in rat hippocampus. *Journal of Neurophysiology, 83*, 2138–2144.